Supporting Information

Elucidating the Effect of Ag Interlayer Formation on the Intrinsic Mechanical Properties of Free-standing ITO/Ag/ITO Thin Films

Seung Jin Oh, Sangmin Lee, Kyung Cheol Choi, Jeong Hyun Kwon, and Taek-Soo Kim**

Seung Jin Oh, Sangmin Lee, and Taek-Soo Kim
[†]Department of Mechanical Engineering, Korea Advanced Institute of Science and Technology (KAIST), Daejeon 34141, Republic of Korea

Kyung Cheol Choi
[‡]School of Electrical Engineering, Korea Advanced Institute of Science and Technology (KAIST), Daejeon 34141, Republic of Korea

Jeong Hyun Kwon
[§]Department of Display and Semiconductor Engineering, Sun Moon University, Asan 31460, Republic of Korea

**Address correspondence to love6539@sunmoon.ac.kr, tskim1@kaist.ac.kr.*

Table S1. Summary of mechanical properties of the IAI thin films with different Ag thicknesses.

Reference	IAI(8)	IAI(10)	IAI(11)	IAI(12)	IAI(13)	IAI(14)	IAI(25)	IAI(50)
Young's modulus (GPa)								
100.3 ± 3.5	74.3 ± 5.6	83.4 ± 0.7	87.1 ± 2.2	85.5 ± 3.7	94.9 ± 3.8	92.8 ± 2.2	77.7 ± 3.7	63.5 ± 9.6
Elongation (%)								
0.27 ± 0.06	0.31 ± 0.01	0.50 ± 0.01	0.44 ± 0.04	0.56 ± 0.12	0.54 ± 0.16	0.57 ± 0.08	0.35 ± 0.08	0.31 ± 0.09
Tensile strength (MPa)								
264.6 ± 60.2	232.7 ± 34.8	419.8 ± 9.8	384.9 ± 37.5	480.0 ± 114.1	514.2 ± 128.1	514.3 ± 71.5	269.3 ± 74.1	195.2 ± 72.4

Table S2. Summary of electrical and optical properties of the IAI thin films with different Ag thicknesses.

IAI(8)	IAI(10)	IAI(11)	IAI(12)	IAI(13)	IAI(14)	IAI(25)	IAI(50)
			Sheet resistance (Ω/sq.)				
110.48 ± 4.64	9.35 ± 0.04	7.87 ± 0.10	4.92 ± 0.01	6.38 ± 0.01	5.81 ± 0.02	1.68 ± 0.02	1.63 ± 0.04
			Transmittance at 550 nm (%)				
70.87	77.63	79.89	83.18	81.69	81.24	60.93	19.75
			Figure of merit (10^{-3}/Ω)				
0.29	8.50	13.46	32.21	20.74	21.54	4.21	5.55×10^{-5}

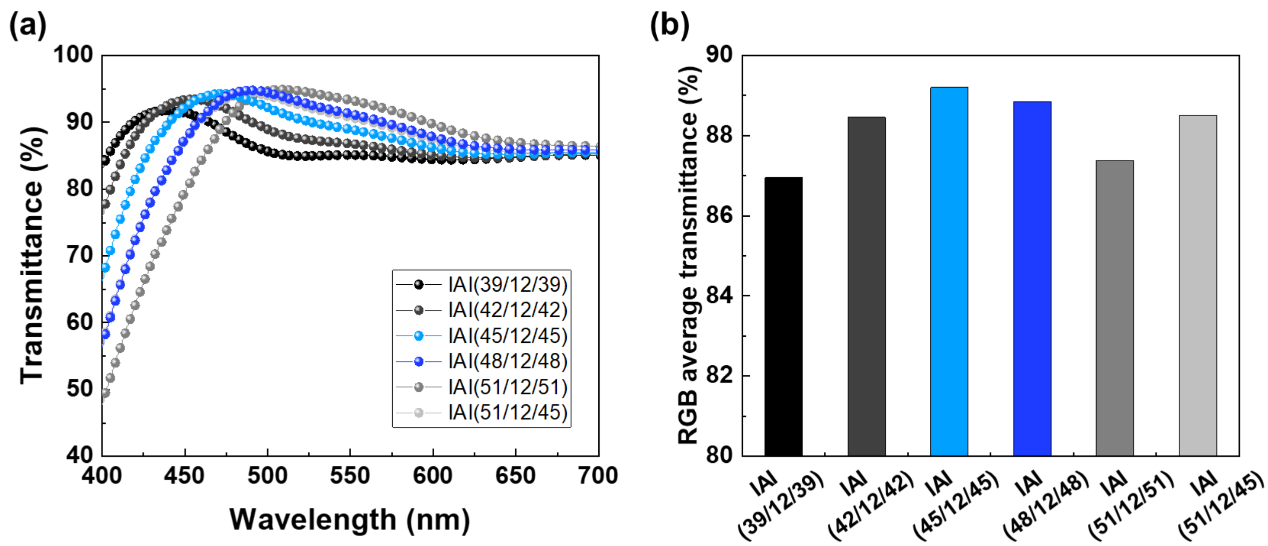

Figure S1. Optical simulation for the varying ITO/Ag/ITO (IAI) multilayer structure. (a) Simulation results. (b) RGB average transmittance values.

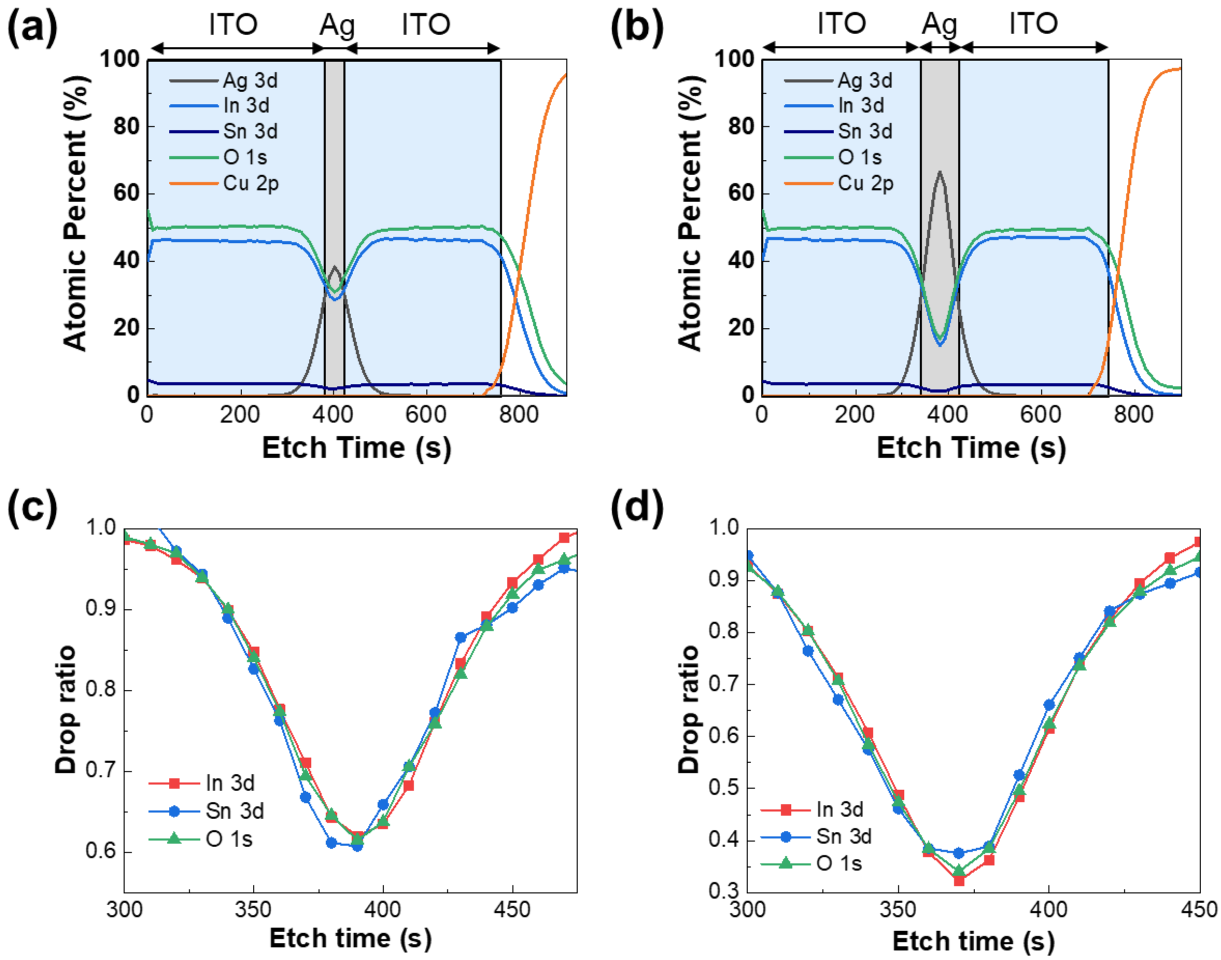

Figure S2. XPS depth profiles of (a) IAI(8) and (b) IAI(12) thin films on the Si substrate. The atomic percent drop ratio of each atom near the Ag interlayer for (c) IAI(8) and (d) IAI(12). The drop ratio was defined as (atomic percent/atomic percent at 100–200 s of etch time).

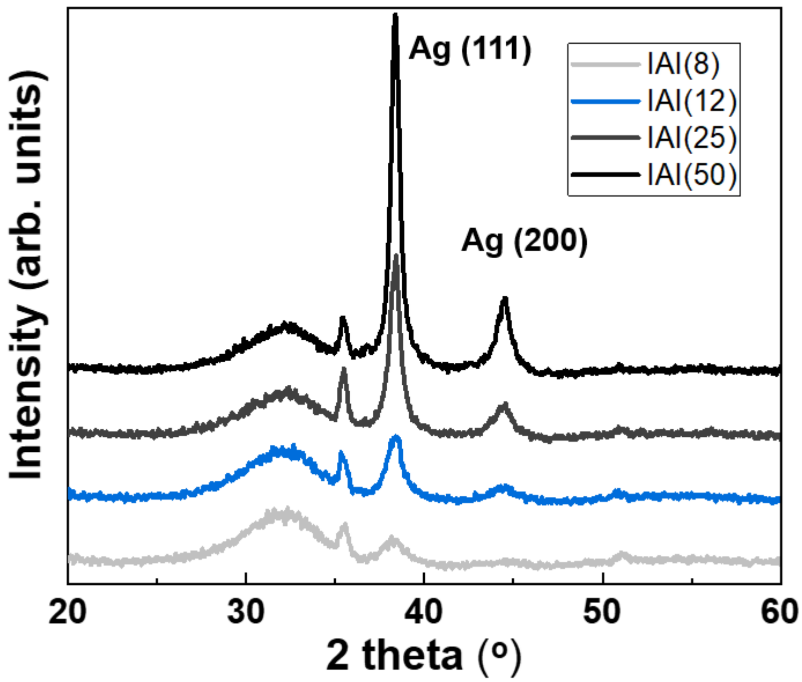

Figure S3. XRD spectra of the IAI thin films as a function of Ag thickness.

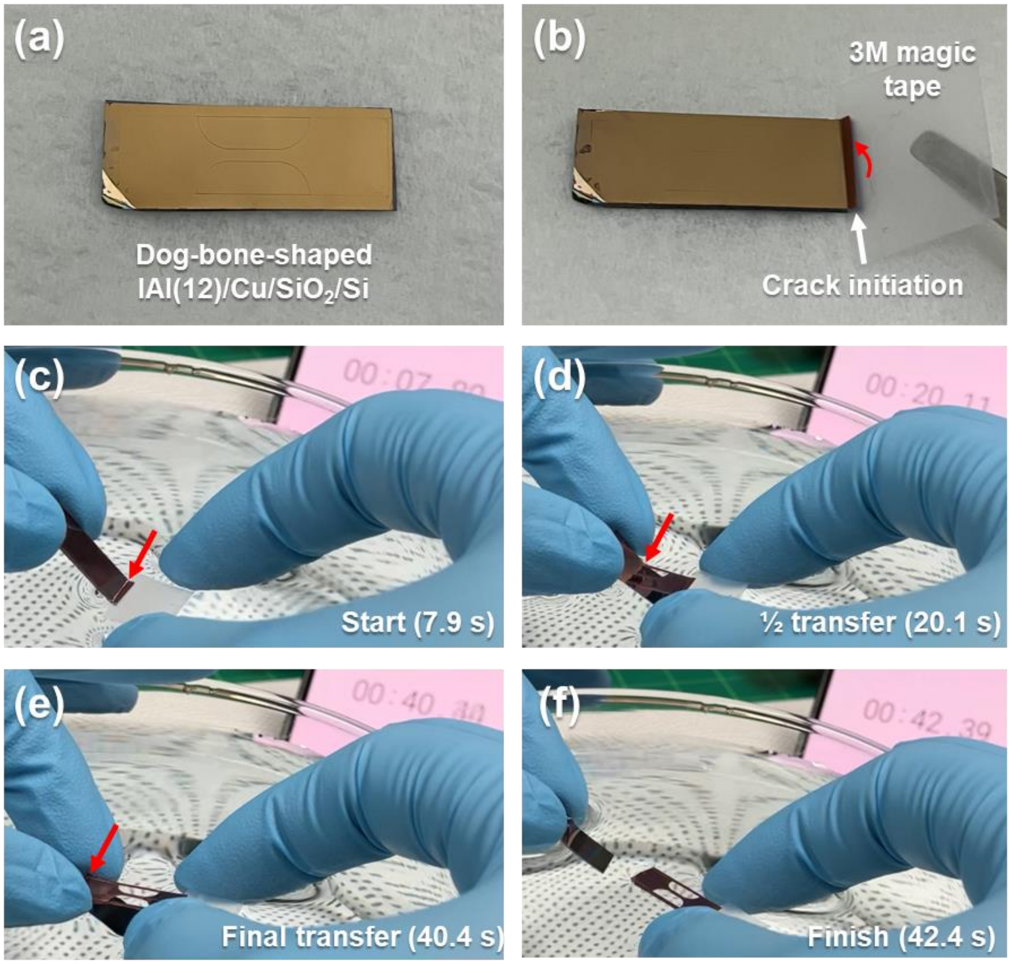

Figure S4. Transfer process of the IAl/Cu bilayer onto the water surface. (a) Prepared sample. (b) Crack initiation of the sample. (c) Beginning of the IAl/Cu bilayer transfer (7.9 s). (d) Middle step of the transfer (20.1 s). (e) The final step of the transfer (40.4 s). (f) Fully-separated dog-bone-shaped sample (42.4 s).

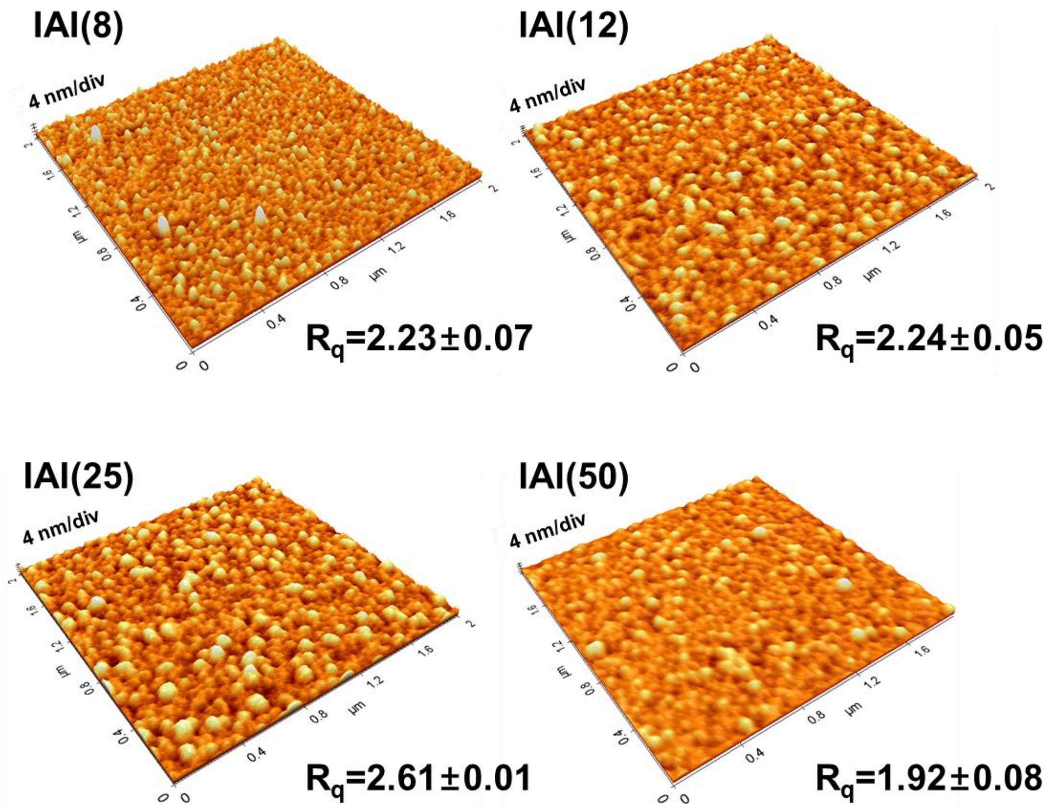

Figure S5. AFM images of the IAI thin films as a function of Ag interlayer thickness. A square area of 2 × 2 µm was scanned.

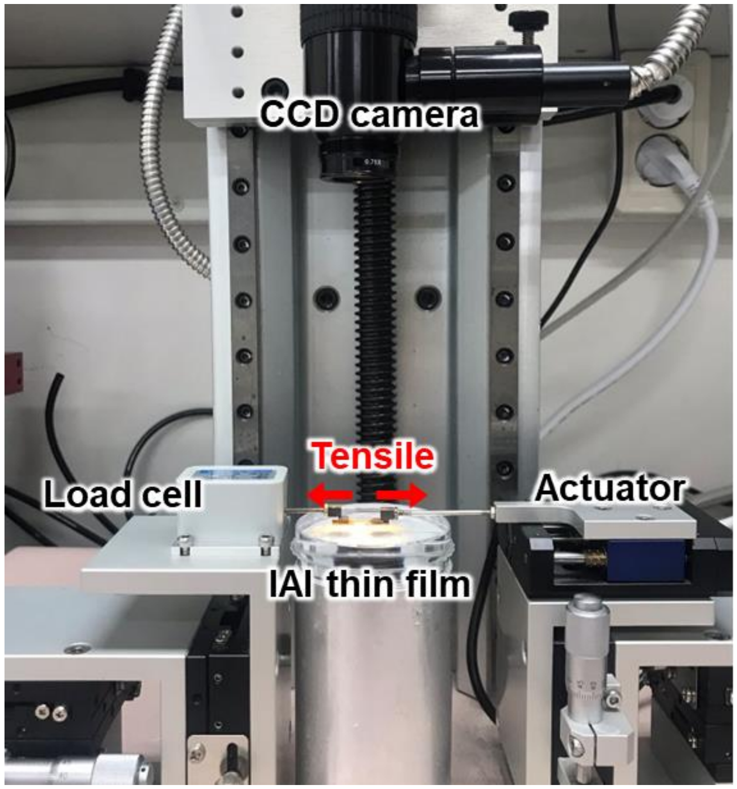

Figure S6. Tensile testing system using water surface platform for the IAI thin films.

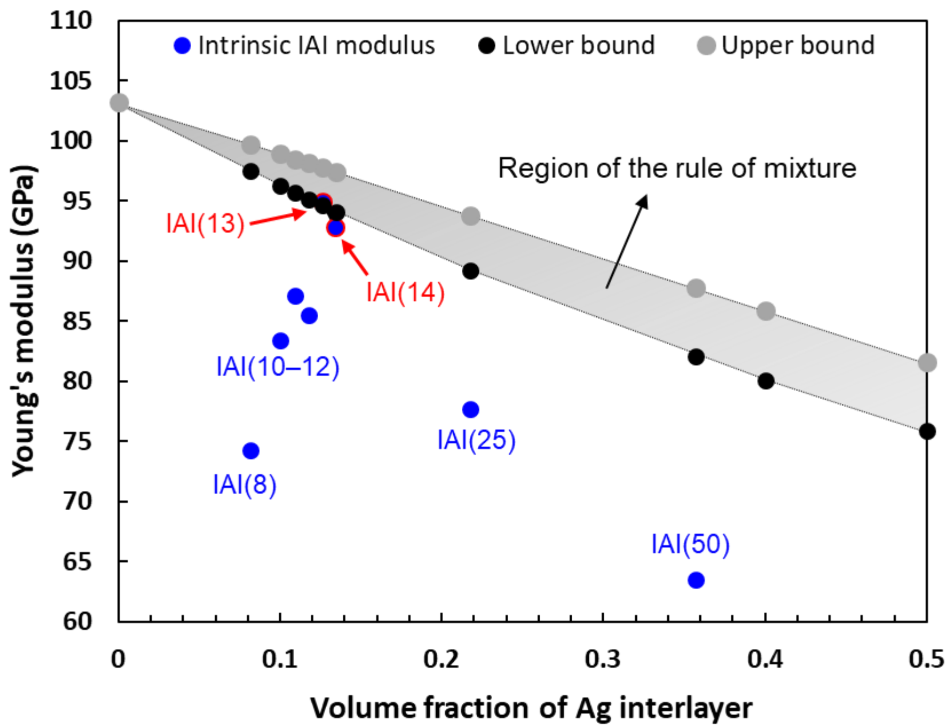

Figure S7. Intrinsic Young's modulus of the IAI thin films as a function of Ag interlayer thickness. The IAI thin films were assumed as the ideal tri-layer to calculate Young's modulus using the rule of mixture. The IAI(13) and IAI(14) with film-like Ag interlayer showed comparable Young's modulus to that calculated by the rule of mixture.

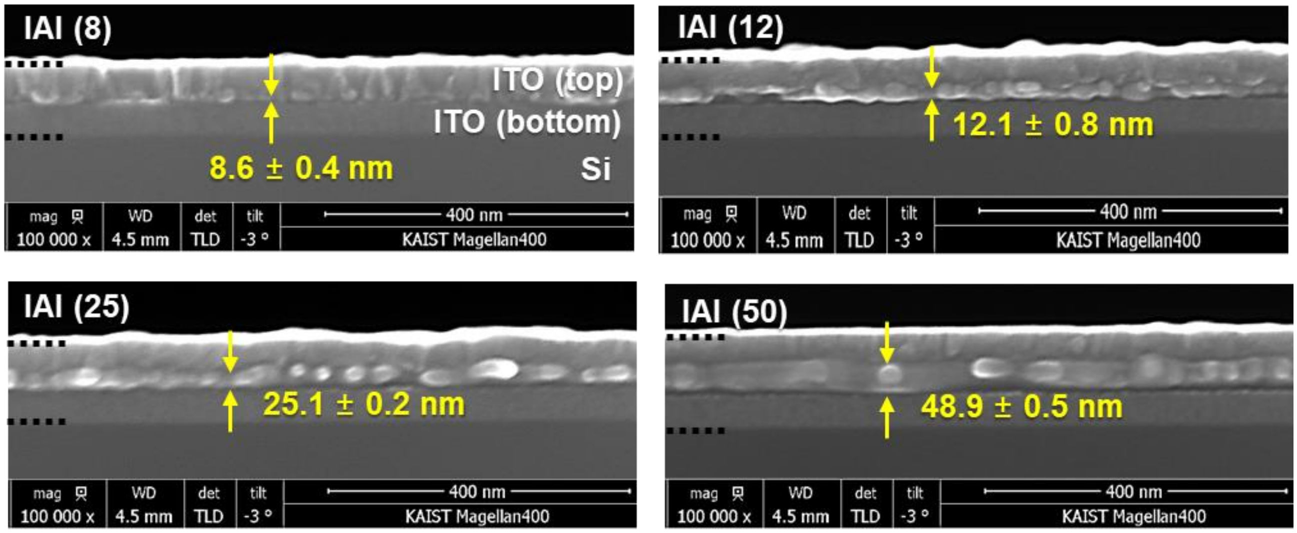

Figure S8. Thicknesses of Ag interlayers of IAI(8), (12), (25), and (50) measured by SEM images.

Three images were analyzed for each sample.

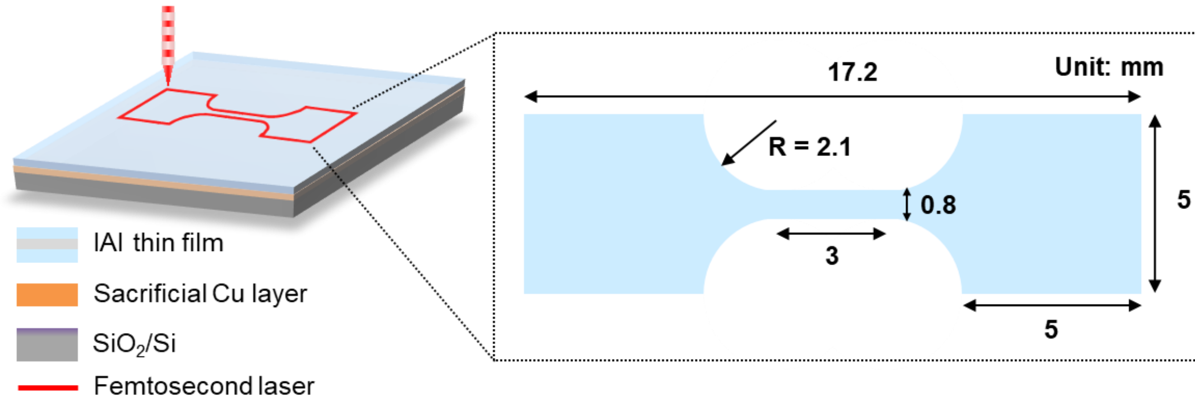

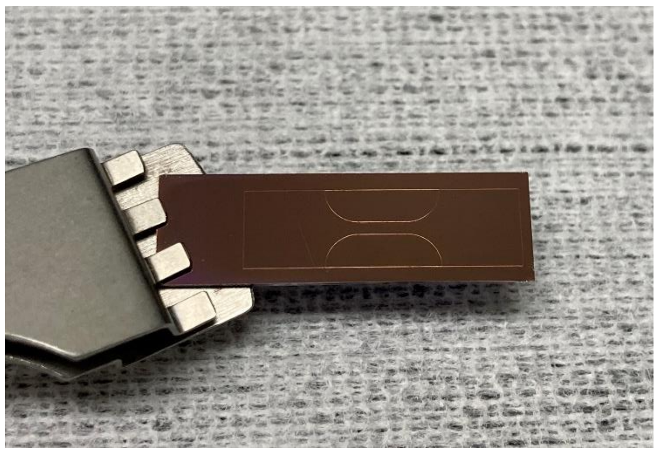

Figure S9. Dimension of the femtosecond laser patterned IAI samples. The photo represents the femtosecond laser patterned IAI sample.

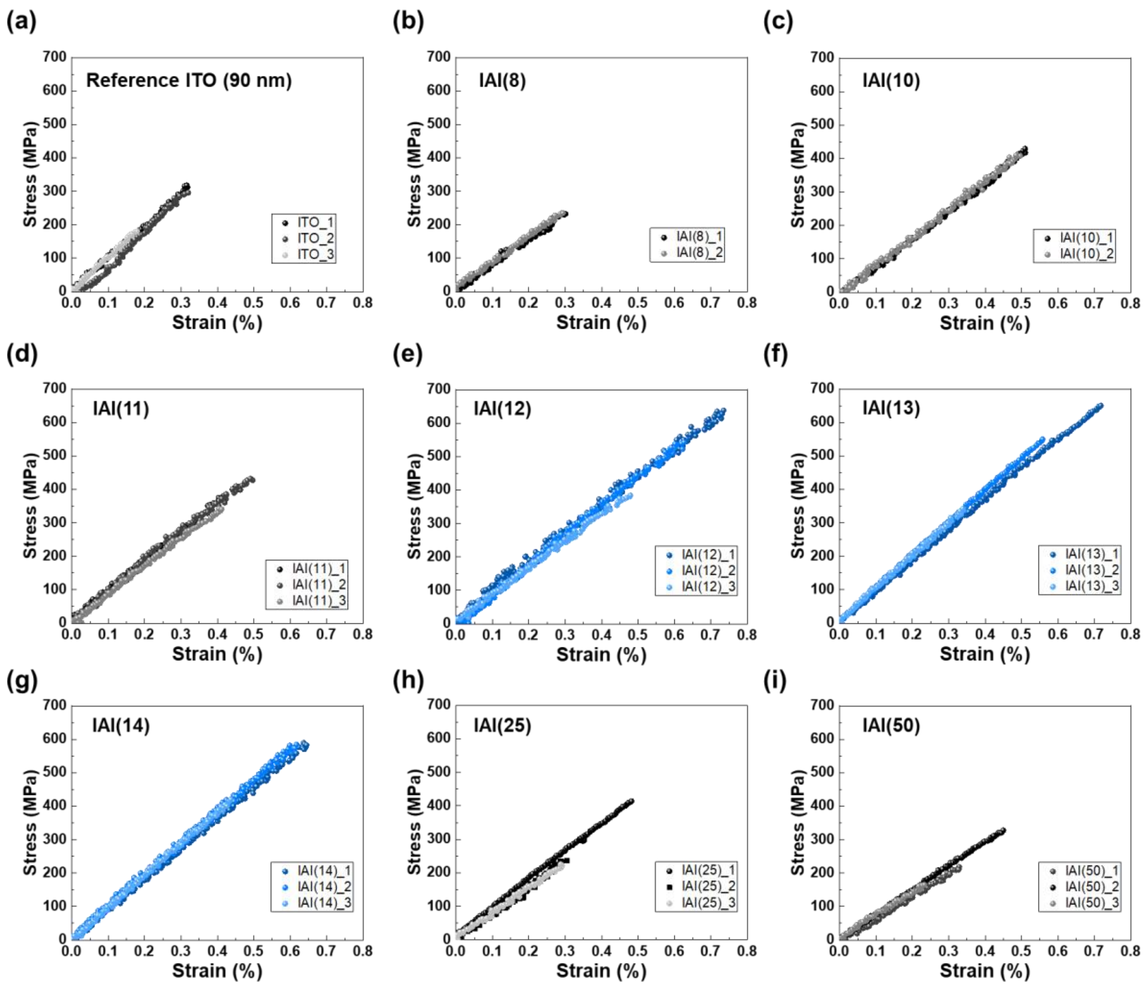

Figure S10. Stress–strain curves as a function of Ag thickness. (a) Reference ITO thin film. (b-i) IAI(8), IAI(10), IAI(11). IAI(12), IAI(13), IAI(14), IAI(25), and IAI(50) thin films.

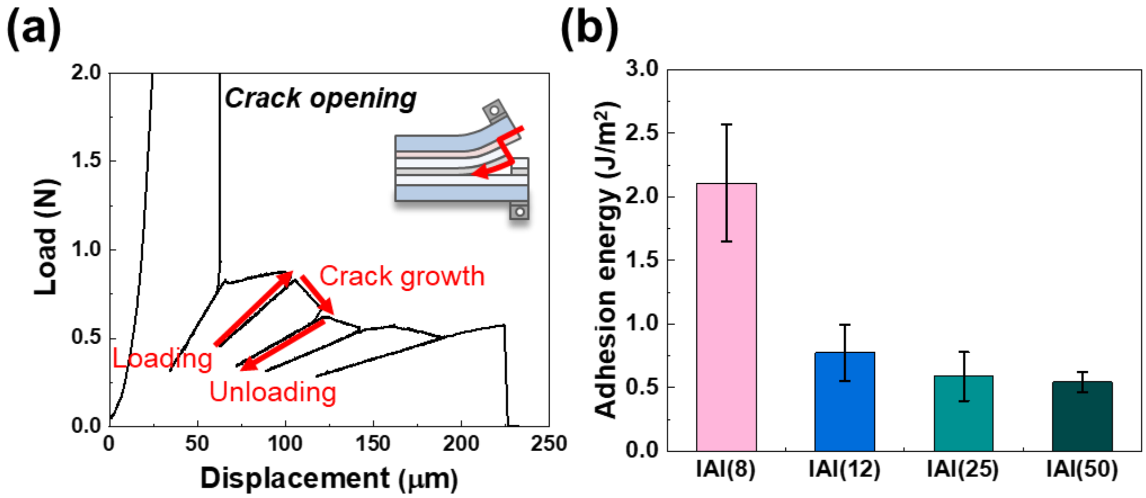

Figure S11. (a) A representative load-displacement curve showing the DCB test procedure including cyclic loading, crack growth, and unloading. (b) Measured mode I adhesion energy of the IAI specimens. The IAI(8) represents the adhesion energy between the epoxy/ITO interface and others represent the adhesion between ITO/Ag interface.